The Journal of the Astronautical Sciences, Vol. 37, No. 4, October-December 1989, pp. 433–450

Annihilation of Angular Momentum Bias During Thrusting and Spinning-up Maneuvers[1]

J. M. Longuski[2], T. Kia[3] and W. G. Breckenridge[3]

Abstract

During spinning-up and thrusting maneuvers of rockets and spacecraft, undesired transverse torques (from error sources such as thruster misalignment, center-of-mass offset and thruster mismatch) perturb the angular momentum vector from its original orientation. In this paper a maneuver scheme is presented which virtually annihilates the angular momentum vector bias, even though the magnitude and direction of the perturbing body-fixed torques are unknown. In the analysis it is assumed that the torques are small and constant and that the spacecraft or rocket can be approximated by a rigid body, which may be asymmetric. Typical maneuvers of the Galileo spacecraft are simulated to demonstrate the technique.

Introduction

Rockets and spacecraft are often spun up to provide stability. The angular momentum vector remains inertially fixed, unless acted upon by an external torque.

When a spinning rocket performs an axially-thrusting maneuver, however, there are always body-fixed torques due to various error sources such as thruster misalignment and center-of-mass offset. An example configuration is illustrated in Fig. 1a in which the thruster offset creates a body-fixed torque into the page. The effect of a constant body-fixed transverse torque, M_x, on the orientation of the angular momentum vector, $\mathbf{H}$, in inertial space is illustrated in Fig. 2a, where XYZ represent inertial coordinates. If the initial orientation of the angular momentum vector is $\mathbf{H}_0$ and the body axis x coincides with the space axis X at the commencement of the maneuver, then the angular momentum vector traces a circular path in inertial space. The average orientation of $\mathbf{H}$ is given by the angle ρ_0 which is in the YZ plane. As a conse-

[1]An early version of this paper was presented at the AAS/AIAA Astrodynamics Conference, Lake Placid, New York, August 22–25, 1983.

[2]Assistant Professor, School of Aeronautics and Astronautics, Purdue University, West Lafayette, IN 47907.

[3]Members of Technical Staff, Jet Propulsion Laboratory, California Institute of Technology, Pasadena, CA 91109.

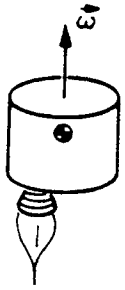

FIG. 1a. The Thrusting Problem.

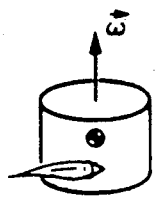

FIG. 1b. The Spinning-Up Problem.

quence, the change of velocity, $\Delta \mathbf{V}$, from the thrusting maneuver is delivered along the same biased orientation. *This is the fundamental mechanism for ΔV pointing errors in axially-thrusting spin-stabilized spacecraft and rockets.*

During spinning-up maneuvers, thruster couples are usually used so that, ideally, only axial torque (and no force) is applied. In practice, however, error sources such as thruster mismatch can lead to a transverse torque. In the case of the Galileo spacecraft, only one thruster is used which results in a large deterministic transverse torque, as illustrated in Fig. 1b. The corresponding behavior of the angular momentum vector in inertial space is shown in Fig. 2b. The angular momentum vector traces out a spiral path about a line in inertial space having an angle ρ_0 from the inertial Z axis and in the YZ plane. After the completion of the spin-up maneuver and the damping out of nutation, the vehicle will have an attitude error or bias of angle ρ_0.

In this paper, a maneuver scheme is presented which virtually annihilates the angular momentum vector bias, ρ_0, for both spinning-up and thrusting maneuvers. By breaking the maneuver up into two "burns" with a "coast" or delay time in between, the bias angle, ρ_0, can be reduced to zero. In the first part of the "two burn" scheme the angu-

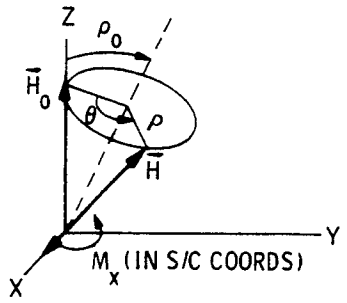

FIG. 2a. The Angular Momentum Vector During Thrusting.

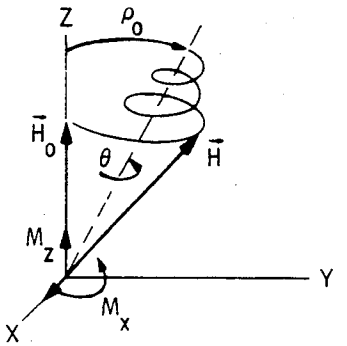

FIG. 2b. The Angular Momentum Vector During Spinning-Up.

lar momentum vector begins to move in a circle or spiral, as before, but then the thruster is turned off. Without any external torques the angular momentum vector becomes stationary in inertial space, but the vehicle continues to spin. When the thruster reaches the appropriate orientation the second "burn" causes the angular momentum vector to encircle the inertial Z axis. The appropriate burn and coast times are given by a transcendental equation similar to Kepler's time equation. The equation only requires knowledge of the initial spin rate and the axial angular acceleration. Knowledge of the transverse torques is not required, but they are assumed to be small and constant.

The paper is organized as follows. First, analytic solutions for the behavior of the angular momentum vector are briefly reviewed. Next the thrusting problem at constant spin rate is discussed and the effect of the two-burn scheme is demonstrated. Finally, the application of the two-burn scheme to the spinning-up problem is discussed and conclusions are drawn.

Analytic Solutions

A Simple Model for the Angular Momentum Vector

Considerable insight can be gained by working directly with Euler's law,

$$\mathbf{M} = \dot{\mathbf{H}} \tag{1}$$

Assume the spin rate, Ω, is constant and that the transverse body-fixed torques M_x and M_y are constant and remain in the inertial XY plane (Fig. 2a). Then equation (1) becomes

$$\dot{H}_X = M_X = M_x \cos \Omega t - M_y \sin \Omega t \tag{2}$$

$$\dot{H}_Y = M_Y = M_x \sin \Omega t + M_y \cos \Omega t \tag{3}$$

$$\dot{H}_Z = 0 \tag{4}$$

where XYZ refer to inertial coordinates and xyz refer to body coordinates. For the initial conditions $H_X(0) = H_Y(0) = 0$ and $H_Z(0) = I_z\Omega$ the integration of equations (2)–(4) provides

$$H_X = (M_x/\Omega) \sin \Omega t + (M_y/\Omega)(\cos \Omega t - 1) \tag{5}$$

$$H_Y = (M_x/\Omega)(1 - \cos \Omega t) + (M_y/\Omega) \sin \Omega t \tag{6}$$

$$H_Z = I_z\Omega \tag{7}$$

Equations (5)–(7) indicate that when $M_y = 0$, the angular momentum vector follows the circular path in space described by Fig. 2a.

This simple model is useful in providing the correct behavior of the angular momentum vector for constant spin rate, but it has serious limitations. There is no indication of stability. The equations do not distinguish between spinning about the principal axes of minimum, intermediate or maximum moment-of-inertia. Another problem is that the equations give no hint as to the allowable size of the bias angle, ρ_0, of Fig. 2a. Finally, the extension to the spinning-up maneuver is not clear, for if the M_x and M_y torques are assumed to remain in the XY plane then should not the M_z torque remain along the Z axis? If this assumption is made, then an incorrect result is obtained

for the spinning-up maneuver, because it will be demonstrated that the angular momentum vector increases along the line indicated by the angle ρ_0 in Fig. 2b.

The formal approach of solving Euler's equations of motion, finding the Eulerian angles and obtaining the angular momentum vector will be described next.

Euler's Equations of Motion

Euler's equations of motion are

$$M_x = I_x\dot{\omega}_x + (I_z - I_y)\omega_y\omega_z \tag{8}$$

$$M_y = I_y\dot{\omega}_y + (I_x - I_z)\omega_z\omega_x \tag{9}$$

$$M_z = I_z\dot{\omega}_z + (I_y - I_x)\omega_x\omega_y \tag{10}$$

By assuming a near-symmetric rigid body, $I_x \approx I_y$, subject to constant torques, M_x, M_y, and M_z, the spin rate is found to vary linearly with time,

$$\omega_z \approx \frac{M_z}{I_z}t + \omega_{z0} \tag{11}$$

and the solution of equations (8) and (9) can be found in terms of Fresnel integrals [1, 2]. In [3, 4] these solutions were found to be relatively insensitive to variations in I_x and I_y, provided that the orientation changes in **H** were small. This is because the last term of equation (10) remains small for stable motion, since the product $\omega_x\omega_y$ remains small. Under these conditions, which are usually representative of practical spacecraft and rocket motion, the solution applies to asymmetric bodies. In [5], Price found the solution of [1] to be a useful first order approximation in his semi-analytic solution of Euler's equations of motion. When $I_x = I_y$, equation (11) becomes exact, so that the solution of Bödewadt for symmetric rigid bodies can be applied [6, 7]. When $M_z = 0$, approximate analytic solutions are easily derived for the asymmetric case by assuming $\omega_z \approx \omega_{z0}$.

Euler's Angles

Twelve forms of Euler angle rotation representations are available to provide the attitude of a rigid body. If a Type 1: 3-1-2 rotation is used [8] then the kinematic equations are

$$\dot{\phi}_x = \omega_x \cos\phi_y + \omega_z \sin\phi_y \tag{12}$$

$$\dot{\phi}_y = \omega_y - (\omega_z \cos\phi_y - \omega_x \sin\phi_y)\tan\phi_x \tag{13}$$

$$\dot{\phi}_z = (\omega_z \cos\phi_y - \omega_x \sin\phi_y)\sec\phi_x \tag{14}$$

By assuming that two of the Eulerian angles ϕ_x and ϕ_y are small, an analytic solution was obtained for equations (12)–(14) in [1] for the case of a near-symmetric rigid body subject to constant body-fixed torques. The solutions for ϕ_x and ϕ_y each contain approximately 75 terms and consist of Fresnel, sine and cosine integrals. The solution for ϕ_z is

$$\phi_z = (1/2)(M_z/I_z)t^2 + \omega_{z0}t + \phi_{z0} \tag{15}$$

A careful numerical study of these solutions [4] shows that they also apply to asymmetric rigid bodies when the motion of the angular momentum vector in inertial space is restricted to very small angles (a few degrees).

Other solutions for the attitude motion of a self-excited rigid body are either incorrect or not explicit. Bödewadt's solution [6, 7] was proven incorrect for the general case in [2]. Armstrong [9] provides very useful observations for limiting cases for symmetric bodies, but does not give explicit solutions.

Formal Solutions for the Angular Momentum Vector

When analytic expressions are available for Euler's equations of motion and the Eulerian angles, then the angular momentum vector in inertial space can be obtained from

$$\begin{bmatrix} H_X \\ H_Y \\ H_Z \end{bmatrix} = \begin{bmatrix} c\phi_z c\phi_y - s\phi_z s\phi_x s\phi_y & -s\phi_z c\phi_x & c\phi_z s\phi_y + s\phi_z s\phi_x c\phi_y \\ s\phi_z c\phi_y + c\phi_z s\phi_x s\phi_y & c\phi_z c\phi_x & s\phi_z s\phi_y - c\phi_z s\phi_x c\phi_y \\ -c\phi_x s\phi_y & s\phi_x & c\phi_x c\phi_y \end{bmatrix} \begin{bmatrix} I_x\omega_x \\ I_y\omega_y \\ I_z\omega_z \end{bmatrix} \tag{16}$$

where c and s denote cosine and sine and Type 1: 3-1-2 Euler angles have been assumed. In the analytic solutions which are being considered, the angles ϕ_x and ϕ_y are small so that equation (16) becomes

$$\begin{bmatrix} H_X \\ H_Y \\ H_Z \end{bmatrix} = \begin{bmatrix} \cos\phi_z & -\sin\phi_z & \phi_y\cos\phi_z + \phi_x\sin\phi_z \\ \sin\phi_z & \cos\phi_z & \phi_y\sin\phi_z - \phi_x\cos\phi_z \\ -\phi_y & \phi_x & 1 \end{bmatrix} \begin{bmatrix} I_x\omega_x \\ I_y\omega_y \\ I_z\omega_z \end{bmatrix} \tag{17}$$

The Thrusting Problem

In the thrusting problem, a spinning rocket or spacecraft uses an axial thruster to provide a change of velocity. An example of this maneuver is found in the Galileo spacecraft (see Fig. 3). Before performing an axial maneuver, the dual-spin spacecraft locks up the rotor and stator so that the vehicle behaves as a single spinner. Then the 10 Newton -Z thrusters may be used. If the 400 Newton engine is to be used, the vehicle is spun up from 3 rpm to 10 rpm with an S thruster in order to provide greater stability.

During the axial maneuver, transverse torques (from error sources such as thruster misalignment and offset, center-of-mass offset and thruster mismatch) lead to velocity pointing errors [10]. Spin rate changes are also expected due to jet damping, primarily in the 400 Newton engine, and misalignments in the 10 Newton thrusters. The spin rate changes are small enough so that the spin rate can be considered constant in the analysis of the velocity pointing errors.

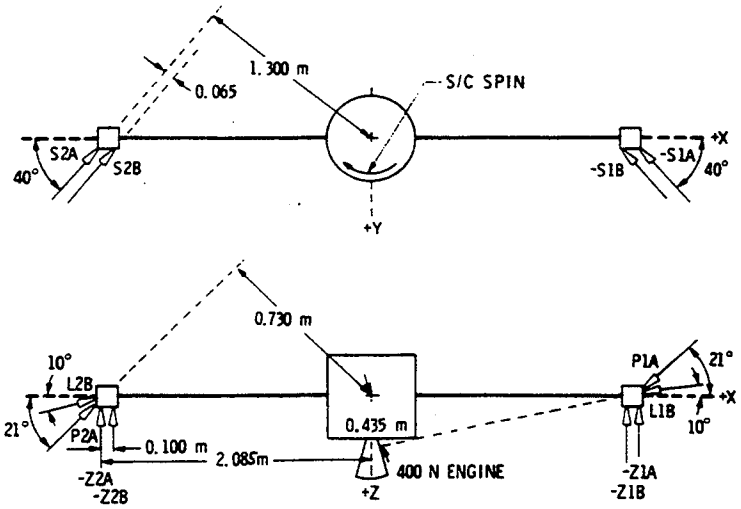

FIG. 3. Galileo Thruster Configuration.

The Behavior of the Angular Momentum Vector During Thrusting

By assuming a constant spin rate about the z axis ($\omega_z = \Omega$), retaining the distinction between I_x and I_y and assuming small angles for ϕ_x and ϕ_y, the analytic integration of equations (8)–(10) and equations (12)–(14) is straightforward. *Combining the results into equation (17) again provides equations (5)–(7) for the behavior of the angular momentum vector.* It is interesting to note that the effects of asymmetry do not appear in these approximate solutions for the angular momentum vector. It is well-known that the solutions for the Euler velocities ω_x and ω_y are stable when

$$I_z > I_x, \qquad I_z > I_y \tag{18}$$

or

$$I_z < I_x, \qquad I_z < I_y \tag{19}$$

Obviously equations (18) and (19) imply

$$I_z \neq I_x \quad \text{and} \quad I_z \neq I_y \tag{20}$$

The conditions (18) or (19) are also required for stability of the ϕ_x and ϕ_y solutions.

It is convenient to define angles ρ_X and ρ_Y to specify the orientation of the angular momentum vector in inertial space:

$$\tan \rho_X = H_X/H_Z \tag{21}$$

$$\tan \rho_Y = H_Y/H_Z \tag{22}$$

Since ρ_X and ρ_Y are assumed small, equations (5)–(7), (21) and (22) provide

$$\rho_X = (M_x/I_z\Omega^2) \sin \Omega t + (M_y/I_z\Omega^2)(\cos \Omega t - 1) \tag{23}$$

$$\rho_Y = (M_x/I_z\Omega^2)(1 - \cos \Omega t) + (M_y/I_z\Omega^2) \sin \Omega t \tag{24}$$

Equations (23) and (24) are simply the equations of a circle with the center located at $(-M_y/I_z\Omega^2, M_x/I_z\Omega^2)$. The angle between the center of the circle and the Z axis is ρ_0,

$$\rho_0 = (M_x^2 + M_y^2)^{1/2}/I_z\Omega^2 \tag{25}$$

as illustrated in Fig. 2a. (Of course in this more general case, the angle ρ_0 is no longer constrained to the YZ plane of the figure.)

Clearly, from equations (23) and (24) the angular radius of the circle, ρ, is equal to ρ_0

$$\rho = \rho_0 \tag{26}$$

The rotation angle, θ, which is illustrated in Fig. 2a is given by

$$\theta = \phi_z = \Omega t \tag{27}$$

where the initial condition for the Eulerian angle, ϕ_{z0}, is assumed to be zero. The equivalence of the Eulerian angle, ϕ_z, and the rotation angle of the angular momentum vector, θ, has important consequences in the control of the angular momentum vector orientation.

The Velocity Equations

The change of velocity in inertial space during thrusting can be found through the acceleration equation

$$\begin{bmatrix} a_X \\ a_Y \\ a_Z \end{bmatrix} = A \begin{bmatrix} f_x/m \\ f_y/m \\ f_z/m \end{bmatrix} \tag{28}$$

where X, Y and Z represent inertial coordinates, A is the matrix in equation (16), f_x, f_y and f_z are body-fixed forces and m is the vehicle mass.

When ϕ_x and ϕ_y are small, the matrix A that appears in equation (28) is equal to the matrix in equation (17). Assuming that the body-fixed forces and vehicle mass are constant, the resulting linear equations can be directly integrated to obtain the components of the velocity change in inertial space, namely ΔV_X, ΔV_Y and ΔV_Z. *Retaining only the secular terms, the results are*

$$\Delta V_X = (f_z/m)[\phi_{y0} + I_x\omega_{x0}(I_z\Omega)^{-1} - M_y(I_z\Omega^2)^{-1}]t \tag{29}$$

$$\Delta V_Y = (f_z/m)[-\phi_{x0} + I_y\omega_{y0}(I_z\Omega)^{-1} + M_x(I_z\Omega^2)^{-1}]t \tag{30}$$

$$\Delta V_Z = (f_z/m)[1 - (f_x/f_z)M_y(I_z - I_x)^{-1}\Omega^{-2} + (f_y/f_z)M_x(I_z - I_y)^{-1}\Omega^{-2}]t \tag{31}$$

where the condition in equation (20) excludes the singularities.

Usually the transverse velocities ΔV_X and ΔV_Y are transformed into velocity pointing errors as in [10], by defining the angles γ_X and γ_Y

$$\tan \gamma_X = \Delta V_X/\Delta V_Z \tag{32}$$

$$\tan \gamma_Y = \Delta V_Y/\Delta V_Z \tag{33}$$

Assuming γ_X and γ_Y are small (a typical requirement in spacecraft design), that the initial conditions are zero and that there are no side forces (f_x and f_y) then equations (29)–(33) provide

$$\gamma_X = -M_y/I_z\Omega^2 \tag{34}$$

$$\gamma_Y = M_x/I_z\Omega^2 \tag{35}$$

The total ΔV pointing error, γ is

$$\gamma = (\gamma_X^2 + \gamma_Y^2)^{1/2} = \rho_0 \tag{36}$$

Thus, the secular velocity pointing error is aligned with the average angular momentum vector orientation. This velocity pointing error was noted in [9] for symmetric bodies.

Controlling the Angular Momentum Vector by a Two-Burn Scheme

In solid lines, Fig. 4 illustrates the behavior of the angular momentum vector in the inertial XY plane when a constant body-fixed torque M_x is present (corresponding to Fig. 2a). (Note that assuming $M_y = 0$ does not affect the generality of the discussion.) For the axially-thrusting maneuver (and perhaps in other applications) the dashed circle in Fig. 4 illustrates the desired final path of the angular momentum vector. From the earlier discussions it is expected that this will result in a very small velocity pointing error.

During the execution of the thrusting maneuver, the initial path of the angular momentum vector will follow the solid line. If the maneuver is interrupted (by shutting down the thruster) at the time that the dashed straight line is intersected, then the angular momentum vector will stop its motion at that point (in inertial space). As shown in Fig. 4, the intersection point is equidistant from the origin and the center of the initial **H** path. The projection of the angular distance, ρ_0, on the X axis is halfway between the origin and the center point so that

$$\rho_0 \cos\theta = \frac{1}{2}\rho_0 \tag{37}$$

Clearly the angular distance cancels. *The fundamental equation for the first burn is*

$$\cos\theta_b = \frac{1}{2} \tag{38}$$

so that

$$\theta_b = 60° \tag{39}$$

Since $\theta = \phi_z = \Omega t$, the burn time of the first burn is simply

$$t_b = \pi/3\Omega \tag{40}$$

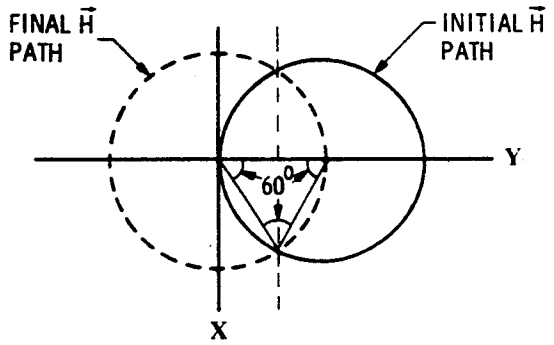

FIG. 4. Initial and Final Paths of the Angular Momentum Vector During the Two-Burn Scheme (for Constant Spin Rate).

In order to achieve the final **H** path the vehicle must be allowed to rotate at the intersection point by a coast angle, θ_c given by

$$\theta_c = \pi - 2\theta_b \tag{41}$$

In this simple case of constant spin rate *the coast angle, θ_c is always*

$$\theta_c = 60° \tag{42}$$

so that the coast time is

$$t_c = \pi/3\Omega \tag{43}$$

At the end of the coast time, the thruster is reignited and the entire maneuver is completed. This completes the two-burn scheme for the thrusting problem (and all other constant spin rate problems).

Numerical Results for the Thrusting Problem

Representative numbers from the Galileo spacecraft [10] can be used to demonstrate the application of the two-burn scheme to the thrusting problem. A 0.02 m center-of-mass offset (3σ) is a typical value for the 400 Newton engine. For convenience, the corresponding torque is assumed to be along the x axis:

$$M_x = (400 \text{ N})(0.02 \text{ m}) = 8 \text{ Nm} \tag{44}$$

As mentioned above, knowledge of the direction and magnitude of the torque is not required for the two-burn scheme to work. The only requirements are that the body-fixed torque remains constant and provides a small value for ρ_0 (e.g., less than 0.5 radians for the near-symmetric case). In this example, assuming Ω = 10 rpm = 1.047 r/s and I_z = 4627 kg–m^2 then

$$\rho_0 = 8 \text{ Nm}(4627 \text{ kg–m}^2)^{-1}(1.047 \text{ r/s})^{-2} = 1.6 \text{ mrad} \tag{45}$$

In the demonstration which follows the values I_x = 3012 kg–m^2, I_y = 2761 kg–m^2 and m = 2000 kg will be used.

In Fig. 5a, the orientation of the angular momentum vector in inertial space is simulated for a 60 second maneuver of the 400 Newton engine. The simulation result is from a very accurate numerical integration of the exact nonlinear equations (8)–(10) and (12)–(14) and the application of the transformation (16). Note the average offset of 1.6 mrad in the Y direction. Figure 5b demonstrates the effect of the two-burn scheme, again using the exact equations of motion in the simulation. The result is that the angular momentum vector encircles the origin as planned.

In Fig. 6a, the velocity pointing error is simulated for the thrusting maneuver.The velocity is found by a precise numerical integration of the exact acceleration equations (28). Note that the transient motion of the velocity vector pointing error is different from the behavior of the corresponding angular momentum vector in Fig. 5a because the periodic terms are different, but the secular behavior of the velocity results in the same offset value of ρ_0 = 1.6 mrad in the Y (inertial) direction.

In Fig. 6b the two-burn scheme is simulated in the same manner. Note that the velocity pointing error is virtually annihilated in a few revolutions.

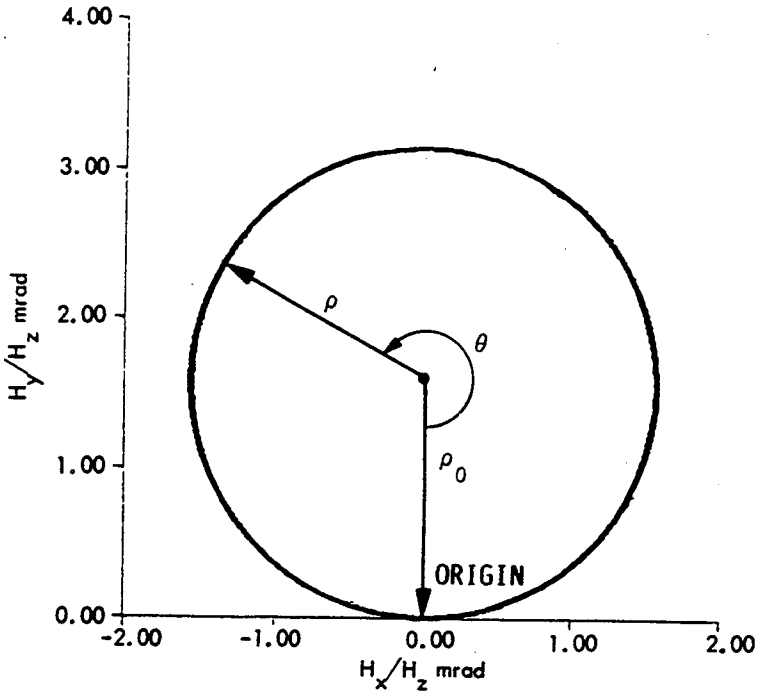

FIG. 5a. Simulation of **H** During Thrusting.

The Spinning-Up Problem

In spinning-up maneuvers of spacecraft and rockets, thruster couples ideally provide a torque precisely along the spin axis without imparting an external force which

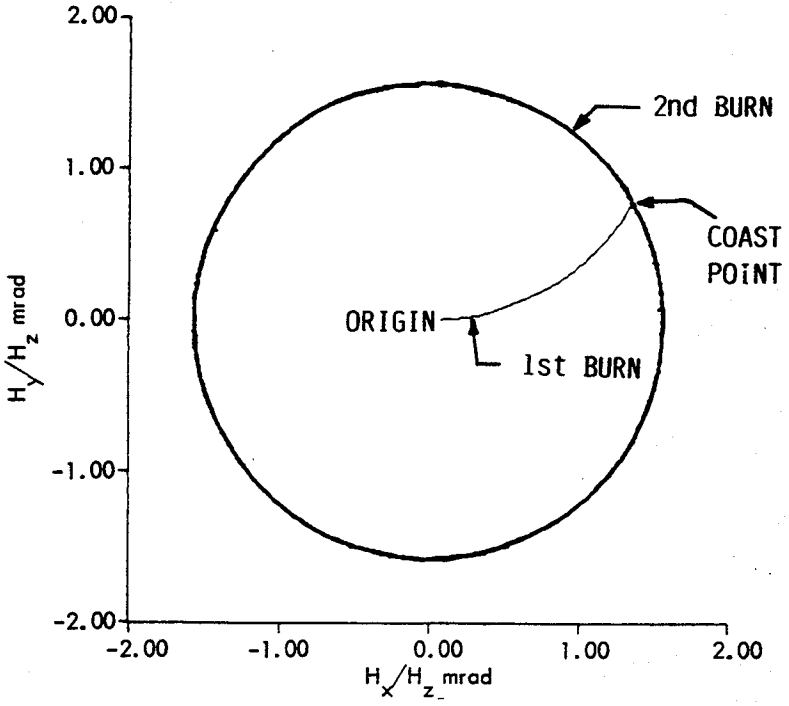

FIG. 5b. Simulation of **H** During Two-Burn Scheme.

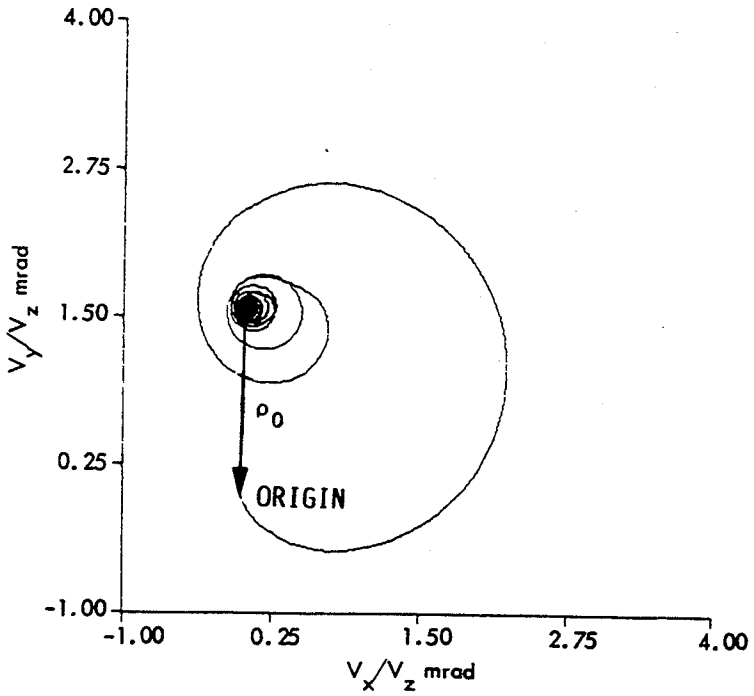

FIG. 6a. Simulation of Velocity Pointing Error During Thrusting.

would change the velocity of the vehicle. In practice, however, thruster mismatch can cause an undesired transverse torque, perturbing the inertial orientation of the angular momentum vector, and an undesired force, which perturbs the velocity. An extreme

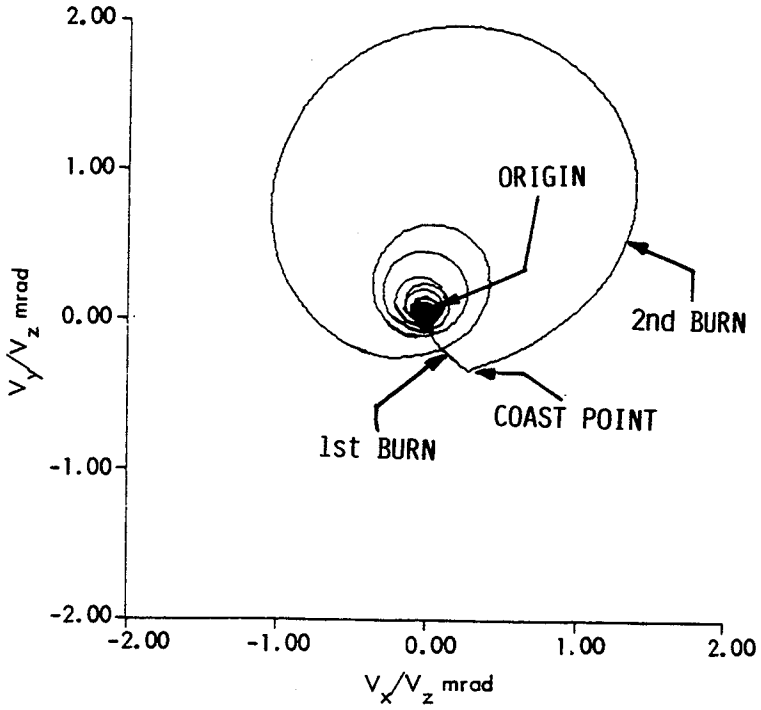

FIG. 6b. Simulation of Velocity During Two-Burn Scheme.

example is the Galileo spacecraft which has a single thruster (the S2A or S2B in Fig. 3) for the spin-up maneuver. Since the spacecraft center-of-mass is not in the xy plane of Fig. 3, there are significant torques about all three body-fixed axes during spin change maneuvers. This example has been an inspiration to the authors to analyze the general problem of the self-excited rigid body [1–4].

The Behavior of the Angular Momentum Vector During Spinning-Up

A very accurate approximate analytic solution for the angular momentum vector is available through equation (17) by using the analytic solutions for Euler's angular velocities and the Eulerian angles [1] where the body is initially spinning about the z axis and conditions (18) or (19) apply. The main restrictions on the solution are that two of the Eulerian angles (ϕ_x and ϕ_y) must remain small, the parameter $|\dot{\omega}_z|/\omega_z^2$ must remain small compared to unity and the body-fixed torques are constant. Under these conditions the solution applies to symmetric and near-symmetric rigid bodies. If the orientation change of the angular momentum vector in inertial space is restricted to less than a few degrees, the solution applies to asymmetric rigid bodies [4].

The analytic solution for the orientation of the angular momentum vector in inertial space is shown in Fig. 7. The parameters are representative of a Galileo spin-up maneuver from 3 rpm to 10 rpm with

$$I_x = 3012 \text{ kg}-\text{m}^2, \qquad I_y = 2761 \text{ kg}-\text{m}^2, \qquad I_z = 5106 \text{ kg}-\text{m}^2 \tag{46}$$

and

$$M_x = -0.4757 \text{ Nm}, \qquad M_y = -0.5669 \text{ Nm}, \qquad M_z = 13 \text{ Nm} \tag{47}$$

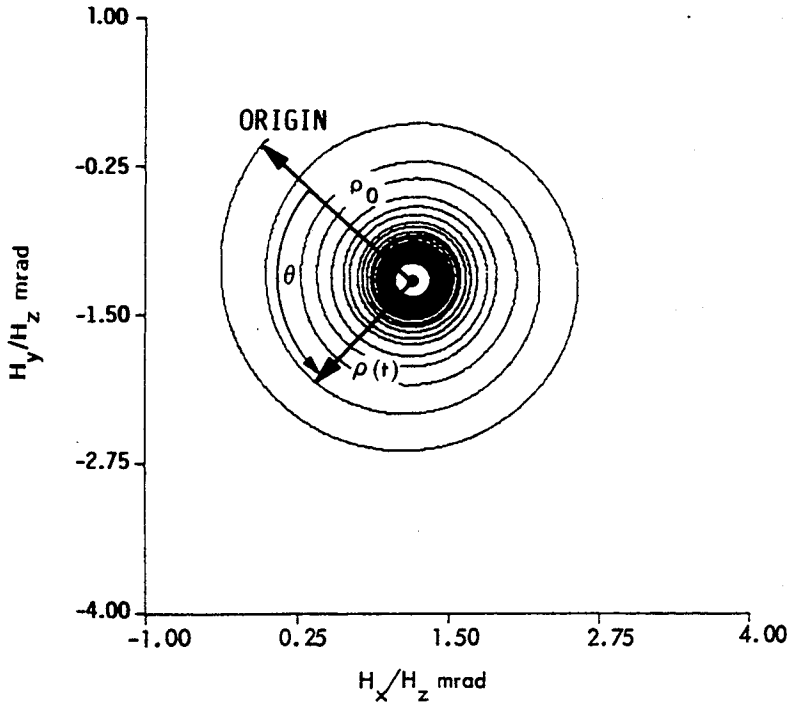

FIG. 7. Orientation of the Angular Momentum Vector During Spinning-Up.

The discrepancy between the exact solution and the analytic solution is not discernible in the figure.

Even though the Eulerian angular velocities and angles exhibit complicated behavior, the behavior of the angular momentum vector is remarkably simple. The distance from the center of the spiral path in Fig. 7 to the origin is given by

$$\rho_0 = (M_x^2 + M_y^2)^{1/2}/I_z\omega_{z0}^2 \tag{48}$$

and the center of the spiral is located at $(-M_y/I_z\omega_{z0}^2, M_x/I_z\omega_{z0}^2)$ which are conditions that are identical to those of the constant spin rate case where $\omega_{z0} = \Omega$. The distance from the origin to any point on the spiral can be approximated by [3, 4]

$$\rho(t) = (M_x^2 + M_y^2)^{1/2}/I_z\omega_z^2(t) \tag{49}$$

where $\omega_z(t)$ is given by equation (11).

This behavior can now be understood by a careful interpretation of equation (1). A first (and naive) approach is to assume that the constant body-fixed transverse torques M_x and M_y remain in the inertial XY plane of Fig. 2b *and that the constant body-fixed spin torque remains aligned with the inertial Z axis*. Assuming that the Euler angle ϕ_z (equation (15)) gives the rotation of the transverse torques in the XY plane, then

$$\dot{H}_X = M_X = M_x \cos\phi_z - M_y \sin\phi_z \tag{50}$$

$$\dot{H}_Y = M_Y = M_x \sin\phi_z + M_y \cos\phi_z \tag{51}$$

$$\dot{H}_Z = M_Z = M_z \tag{52}$$

These equations are analogous to equations (2)–(4). The approach is naive because the analytic integration of equations (50) and (51) produces Fresnel integrals, which are bounded, but the integration of equation (52) results in a secular term. The result would indicate that the orientation of the angular momentum vector asymptotically approaches the inertial Z axis, which is in disagreement with equation (48) and Fig. 7.

Equations (50)–(52) must be adjusted to account for the average orientation of the spin torque in inertial space, which makes an angle of ρ_0 with the Z axis. Incorporating this known behavior into equations (50)–(52) gives

$$\dot{H}_X = M_x \cos\phi_z - M_y \sin\phi_z - M_yM_z/(I_z\omega_{z0}^2) \tag{53}$$

$$\dot{H}_Y = M_x \sin\phi_z + M_y \cos\phi_z + M_xM_z/(I_z\omega_{z0}^2) \tag{54}$$

$$\dot{H}_Z = (\cos\rho_0)M_z \approx M_z \tag{55}$$

Equation (55) remains unchanged because ρ_0 is small. Equations (53)–(55) can be analytically integrated to obtain

$$\Delta H_X = M_x\tilde{C} - M_y\tilde{S} - M_yM_zt/(I_z\omega_{z0}^2) \tag{56}$$

$$\Delta H_Y = M_x\tilde{S} + M_y\tilde{C} + M_xM_zt/(I_z\omega_{z0}^2) \tag{57}$$

$$\Delta H_Z = M_zt \tag{58}$$

Asymptotic expansions may be used to evaluate the Fresnel type integrals [11] in equations (56) and (57):

$$\tilde{C} = \int_0^t \cos \phi_z \, dt = \omega_z^{-1} \sin \phi_z - \omega_{z0}^{-1} \sin \phi_{z0} \tag{59}$$

$$\tilde{S} = \int_0^t \sin \phi_z \, dt = -\omega_z^{-1} \cos \phi_z + \omega_{z0}^{-1} \cos \phi_{z0} \tag{60}$$

Assuming initial conditions

$$H_Z(0) = I_z \omega_{z0} \tag{61}$$

and

$$\omega_{x0} = \omega_{y0} = \phi_{x0} = \phi_{y0} = \phi_{z0} = 0 \tag{62}$$

and noting that

$$M_z t = I_z(\omega_z - \omega_{z0}) \tag{63}$$

equations (56)–(63) give

$$H_X = M_x \omega_z^{-1} \sin \phi_z + M_y \omega_z^{-1} \cos \phi_z - M_y I_z \omega_z / I_z \omega_{z0}^2 \tag{64}$$

$$H_Y = -M_x \omega_z^{-1} \cos \phi_z + M_y \omega_z^{-1} \sin \phi_z + M_x I_z \omega_z / I_z \omega_{z0}^2 \tag{65}$$

$$H_Z = I_z \omega_z \tag{66}$$

The orientation of the angular momentum vector in inertial space is obtained from equations (21), (22) and (64)–(66)

$$\rho_X = (M_x / I_z \omega_z^2) \sin \phi_z + (M_y / I_z \omega_z^2) \cos \phi_z - M_y / I_z \omega_{z0}^2 \tag{67}$$

$$\rho_Y = -(M_x / I_z \omega_z^2) \cos \phi_z + (M_y / I_z \omega_z^2) \sin \phi_z + M_x / I_z \omega_{z0}^2 \tag{68}$$

which are analogous to equations (23) and (24). Equations (67) and (68) are in agreement with equation (49) as can be seen from

$$\rho(t) = [(\rho_X + M_y / I_z \omega_{z0}^2)^2 + (\rho_Y - M_x / I_z \omega_{z0}^2)^2]^{1/2} \tag{69}$$

Equations (67) and (68) capture the essential behavior of the angular momentum vector during spinning-up.

Annihilation of the Angular Momentum Vector Bias by a Two-Burn Scheme

Figure 8 depicts the angular momentum vector spiral, with its center on the Y inertial axis. This corresponds to a single body-fixed transverse torque, M_x, as illustrated in Fig. 2b, but this does not limit the generality of the discussion. Note that if the torques are shut off then the angular momentum vector will cease its motion. If the shut-off occurs at the point halfway to the center of the spiral (indicated by the dashed line in Fig. 8), then the angular momentum vector will stop there. If, after a suitable time delay, the torques are turned on again, then the angular momentum vector may be forced to spiral around the origin for the second and final part of the burn. This describes the "two-burn" scheme for the spin-up maneuver.

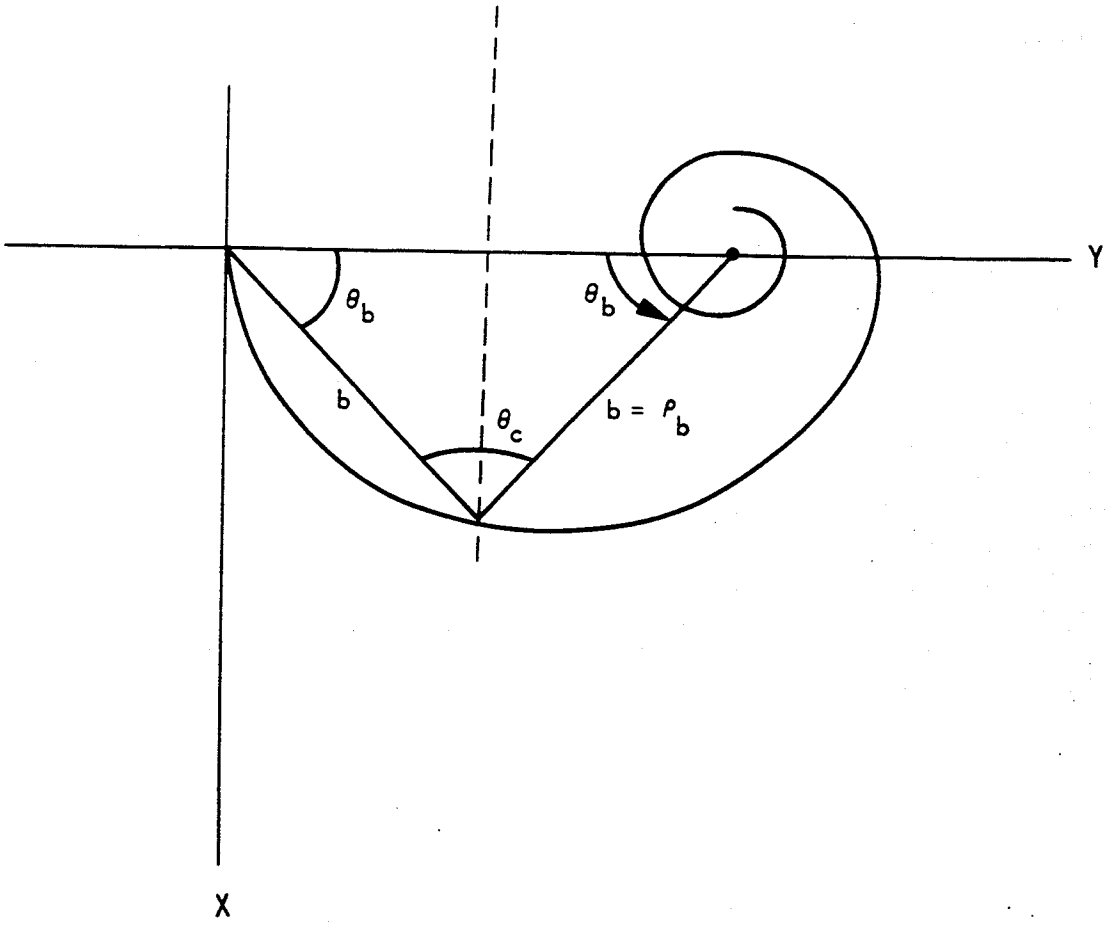

FIG. 8. Analysis of Two-Burn Scheme for Spinning-Up.

The halfway point is reached when

$$\rho_b \cos \theta_b = \rho_0/2 \tag{70}$$

as illustrated in the figure. The value for ρ_b is, from equation (49),

$$\rho_b = (M_x^2 + M_y^2)^{1/2}/I_z\omega_z^2(t_b) \tag{71}$$

where t_b is the duration of the first burn. From equations (67) and (68) it is clear that the rotation angle of the angular momentum vector, θ, is the same as the Euler angle ϕ_z,

$$\theta = \phi_z \tag{72}$$

In compliance with the previous assumptions in equation (62) note that

$$\phi_{z0} = 0 \tag{73}$$

It is convenient to eliminate the time variable between $\omega_z(t)$, in equation (11), and $\phi_z(t)$, in equation (15), so that equation (70) can be written as a function of θ:

$$\omega_z^2 = 2\dot{\omega}_z\phi_z + \omega_{z0}^2 \tag{74}$$

where

$$\dot{\omega}_z = M_z/I_z \tag{75}$$

From equations (48) and (71)–(74), equation (70) becomes

$$(M_x^2 + M_y^2)^{1/2} I_z^{-1} (2\dot{\omega}\theta_b + \omega_{z0}^2)^{-1} \cos\theta_b = (M_x^2 + M_y^2)^{1/2} I_z^{-1} \omega_{z0}^{-2}/2 \tag{76}$$

Rearranging,

$$\cos\theta_b - \dot{\omega}\theta_b \omega_{z0}^{-2} = 1/2 \tag{77}$$

Equation (77) is the fundamental transcendental equation for the two-burn scheme. It is similar in form to Kepler's equation of time. A variety of numerical techniques can be used to find the burn angle, θ_b, which can then be used to find the burn time, t_b, from equation (15). Note that when $\dot{\omega} = 0$, equation (77) reduces to equation (38), so that equation (77) provides the general solution for spin-up and constant spin maneuvers.

After completion of the first burn, the vehicle must rotate through a coast angle, θ_c, in order to achieve the correct phase angle such that the completion of the spin-up maneuver will cause the angular momentum vector to spiral about the origin. From Fig. 8 it is clear that the coast angle is given by

$$\theta_c = \pi - 2\theta_b \tag{78}$$

which is identical to equation (41) for the constant spin rate case. *Equation (78) provides the fundamental equation for the coast angle in the two-burn scheme.* The coast time, t_c, is found by solving equation (15) with the quadratic equation.

After completion of the coasting phase, the second and final burn of the spin-up maneuver will cause the angular momentum vector to spiral about the origin.

Numerical Results for the Spinning-Up Problem

The numerical results for a single burn spin-up maneuver are displayed in Fig. 7 for the parameters in equations (46) and (47).

The efficacy of the two-burn scheme for the spinning-up maneuver can now be tested. Calculations for the first burn and coast provide

$$\theta_b = 58.25° \tag{79}$$

$$t_b = 3.195 \text{ s} \tag{80}$$

$$\theta_c = 63.50° \tag{81}$$

$$t_c = 3.479 \text{ s} \tag{82}$$

The results are shown in Fig. 9. The figure was produced from a very precise numerical integration of the exact equations (8)–(10) and (12)–(14) and the application of the transformation (16). *The figure clearly demonstrates the annihilation of the angular momentum vector bias.*

Conclusions

The two-burn scheme presented here has two important applications: (1) the reduction of velocity pointing errors in axially thrusting rigid body spacecraft spinning at

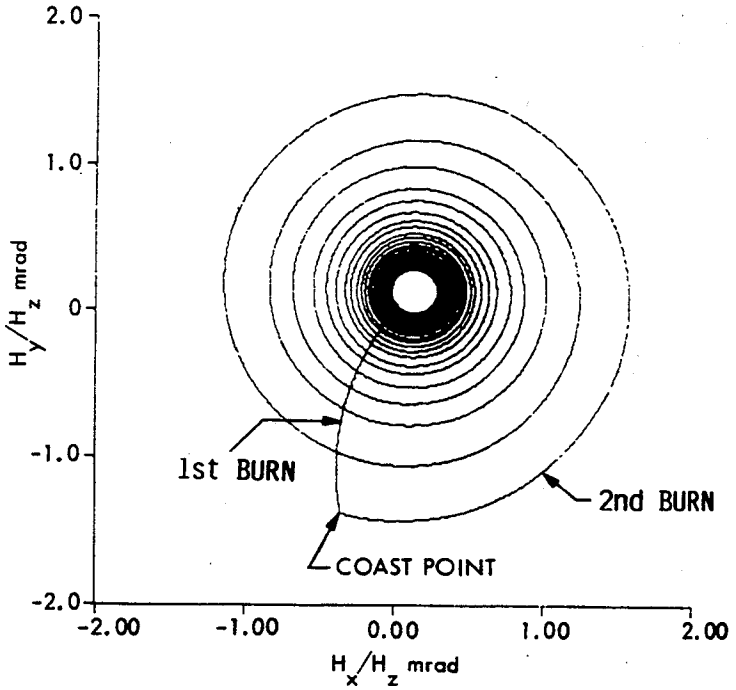

FIG. 9. Annihilation of Angular Momentum Vector Bias During Spinning-Up.

a constant rate and (2) the annihilation of angular momentum vector drift during spinning-up maneuvers. Simple analytic expressions provide the burn and coast times as functions of angular acceleration and initial spin rate. Knowledge of the magnitude and orientation of the disturbing transverse body-fixed torques is unnecessary. Major assumptions are that the thrusters can be turned off and on, that the torques are constant when the thrusters are on, that the vehicle is spinning about a stable principal axis and that two of the Eulerian angles remain small. The technique is most effective when the duration of the maneuver corresponds to several revolutions of the body. The method applies to symmetric, near-symmetric and, under more restrictive conditions, asymmetric rigid bodies.

Acknowledgment

The authors thank John E. McIntyre for his contribution. Part of the research described in this paper was carried out at the Jet Propulsion Laboratory, California Institute of Technology, under contract with the National Aeronautics and Space Administration. Additional support was provided by the National Science Foundation under Grant No. MSS-8908392 (NSF program official Elbert L. Marsh, cognizant NSF grants official Donna C. Jennings).

References

[1] LONGUSKI, J. M. "Solution of Euler's Equations of Motion and Eulerian Angles for Near Symmetric Rigid Bodies Subject to Constant Moments," AIAA Paper 80-1642, AIAA/AAS Astrodynamics Conference, Danvers, Massachusetts, August 11–13, 1980.

[2] LONGUSKI, J. M. "On the Attitude Motion of a Self-Excited Rigid Body," *Journal of the Astronautical Sciences*, Vol. 32, No. 4, October-December 1984, pp. 463–473.

[3] LONGUSKI, J. M. and KIA, T. "A Parametric Study of the Behavior of the Angular Momentum Vector During Spin Rate Changes of Rigid Body Spacecraft," *Journal of Guidance, Control and Dynamics*, Vol. 7, No. 3, May-June 1984, pp. 295–300.

[4] KIA, T. and LONGUSKI, J. M. "Error Analysis of Analytic Solutions for Self-Excited Near Symmetric Rigid Bodies: A Numerical Study," AIAA Paper 84-2018, AIAA/AAS Astrodynamics Conference, Seattle, Washington, August 20–22, 1984.

[5] PRICE, H. L. "An Economical Series Solution of Euler's Equations of Motion, with Application to Space-Probe Maneuvers," Paper 81-105, AAS/AIAA Astrodynamics Conference, Lake Tahoe, Nevada, August 3–4, 1981.

[6] BÖDEWADT, U. T. "Der symmetrische Kreisel bei zeitfester Drehkraft," *Mathematische Zeitschrift*, Vol. 55, 1952, pp. 310–320.

[7] LEIMANIS, E. *The General Problem of the Motion of Coupled Rigid Bodies About a Fixed Point*, Springer-Verlag, New York, 1965.

[8] WERTZ, J. R. *Spacecraft Attitude Determination and Control*, D. Reidel Publishing Company, Dordrecht, Holland, 1980.

[9] ARMSTRONG, R. S. "Errors Associated With Spinning-Up and Thrusting Symmetric Rigid Bodies," Technical Report No. 32-644, Jet Propulsion Laboratory, California Institute of Technology, Pasadena, California, February 15, 1965.

[10] LONGUSKI, J. M. "Galileo Maneuver Analysis," Paper No. 81-137, AAS/AIAA Astrodynamics Conference, Lake Tahoe, Nevada, August 3–5, 1981.

[11] ABRAMOWITZ, M. and STEGUN, I. A. *Handbook of Mathematical Functions*, Dover Publications, Inc., New York, December 1972.